Temperature-dependent concentration quenching and site-dependent effects of Nd^{3+} fluorescence in fluorophosphate glasses

R. Balda and J. Fernández
Departamento de Física Aplicada I, Escuela Técnica Superior de Ingenieros Industriales y de Telecomunicación, Universidad del País Vasco, Alameda de Urquijo s/n 48013 Bilbao, Spain

A. de Pablos and J. M. Fdez-Navarro
Instituto de Cerámica y Vidrio, 28500 Arganda del Rey, Madrid, Spain

M. A. Arriandiaga
Departamento de Física Aplicada II, Facultad de Ciencias, Universidad del País Vasco, Apartado 644, Bilbao, Spain
(Received 20 October 1995)

The optical properties and temperature-dependent concentration quenching of Nd^{3+} fluorescence have been investigated in fluorophosphate glasses with different fluorine to oxygen ratios by using steady-state and time-resolved laser spectroscopy. Judd-Ofelt parameters were derived from the absorption spectra and used to calculate the $^4F_{3/2} \rightarrow {}^4I_{11/2}$ stimulated emission cross section and the $^4F_{3/2}$ radiative lifetime. For the samples doped with 1 wt % of Nd_2O_3 the lifetimes were found to be linear dependent on the fluorine to oxygen ratio. From the thermal behavior of lifetimes, a linear temperature dependence for the nonradiative Nd-Nd relaxation processes has been found in the 4.2–100 K temperature range for samples with a molar fluorine to oxygen ratio of 6.04 doped with more than 1 wt % of Nd_2O_3, which is in agreement with a one-phonon-assisted process. In order to investigate the influence of the local coordination ions on the optical properties of rare earths in these fluorophosphate glasses, fluorescence line-narrowing spectroscopy on Eu^{3+} has been performed. The influence of the local coordination ions on the optical properties of Eu^{3+} in these fluorophosphate glasses shows the existence of a clear crossover between the behavior of fluorinelike and oxygenlike coordination anions.

I. INTRODUCTION

Fluoride phosphate glasses have been a subject of increasing interest in the last few years. Glasses based on fluorides generally have low linear and nonlinear refractive indices, low dispersion, and good transparency from ultraviolet to the infrared region of the optical spectrum.[1,2] These special optical properties make them attractive candidates for applications in high performance optics and laser technology. Together with a high resistance to radiation damage the luminescence characteristics of laser materials are important in order to optimize the output power and efficiency delivered by a solid-state laser system which mainly depend on the loss at the lasing wavelength within the active medium.[3] All of these properties are influenced by glass structure. For a glass laser, the effects of site-to-site variations, in the large-signal gain regime, cause hole burning and reduced energy output. Therefore, the knowledge of the distribution of spectroscopic properties for laser ions in glass is important to select the optimum host glass and operating conditions.[4] In the case of fluorophosphate glasses the structure and related spectroscopic properties mainly depend on the oxygen to fluorine ratio.[1]

A knowledge about the most important laser parameters requires a detailed spectroscopic study of the optical properties of paramagnetic ions, which are influenced by the glass structure.[5] These properties include absorption and emission cross sections, peak wavelengths and linewidths, lifetimes and quantum efficiencies, and fluorescence quenching processes. For a good efficiency, fluorescence lifetimes of Nd^{3+} ions must be close to the calculated radiative lifetime. The lifetime of an excited state is determined by all the competing radiative and nonradiative decay processes; the latter include both Nd-Nd self-quenching and multiphonon relaxation. Concentration quenching and multiphonon emission are dependent on the lasing ion and the glass hosts.[3] In a previous work,[6] some of the authors have studied the luminescence quenching of the $^4F_{3/2} \rightarrow {}^4I_{11/2}$ laser transition in three different fluoride glasses, by investigating the thermal and concentration dependence of lifetimes. Although multiphonon relaxation of the $^4F_{3/2}$ state is negligible for fluoride glasses, at a concentration higher than 1 mol % the experimental lifetime was shorter than the predicted radiative lifetime even at helium temperature. Moreover, from the thermal behavior of lifetimes a T^3 dependence for the nonradiative Nd-Nd relaxation process was found in the 15–100 K temperature range for all the studied samples which is in agreement with a two-site nonresonant process.

The aim of this work is to establish a correlation between glass-matrix composition and Nd^{3+} spectral properties in fluorophosphate glasses with different oxygen to fluorine ratio; in particular, to investigate the nature of the nonradiative Nd-Nd relaxation process in order to compare it with the above mentioned features in pure fluoride matrices. The study includes absorption and emission properties, lifetimes, fluorescence quenching processes, and site-dependent effects. This is followed by a short study of the time-resolved resonant line-narrowed $^5D_0 \rightarrow {}^7F_0$ emission of Eu^{3+} in the glass with a molar fluorine to oxygen ratio of 6.04.

II. EXPERIMENTAL

Fluorophosphate glass samples were obtained with the molar composition $(65\text{-}x)Al(PO_3)_3$-23.44BaF_2-18.75CaF_2-14.06MgF_2-$(37.5+x)AlF_3$ ($x=0$, 1, 2, 2.5, and 3). We have studied five samples with a theoretical molar fluorine to oxygen ratio (F/O) 4, 4.84, 6.04, 6.88, and 8 which have been labeled as glasses *A*, *B*, *C*, *D*, and *E*, respectively. The samples were doped with 1 wt % of Nd_2O_3. Glass *C* was also doped with 0.5, 2, and 5 wt % of Nd_2O_3. They were prepared by melting the precursor mixture in covered platinum crucibles in an electric furnace heated up to 1200 °C under controlled atmosphere. The melt was poured into a preheated brass mould and annealed at 490 °C. Finally the samples were cut and polished for optical measurements.

The samples temperature was varied between 4.2 and 300 K with a continuous-flow cryostat. Conventional absorption spectra were performed with a Cary 5 spectrophotometer. The steady-state emission measurements were made using as exciting light an argon laser and the medium wave tuning range (800–920 nm) of a Ti-sapphire ring laser, pumped by an argon laser. The fluorescence was analyzed with a 0.22 m SPEX monochromator, and the signal was detected by a Hamamatsu R7102 extended IR photomultiplier and finally amplified by a standard lock-in technique.

Lifetime measurements were performed with a tunable dye laser of 9 ns pulse width and 0.08 cm^{-1} linewidth. The emission was detected with a Hamamatsu R7102 photomultiplier. Data were processed by a EGG-PAR boxcar integrator.

The $^5D_0 \rightarrow {}^7F_0$ transition of Eu^{3+} was excited by a pulsed frequency doubled Nd:YAG pumped tunable dye laser of 9 ns pulse width and 0.08 cm^{-1} linewidth. The time-resolved fluorescence was analyzed and detected with a EGG-PAR optical multichannel analyzer.

III. SPECTROSCOPIC RESULTS

A. Absorption properties

The room-temperature absorption spectra were recorded for all samples in the 300–2500 nm spectral range using a Cary 5 spectrophotometer. The spectral resolution of the spectrophotometer was 0.5 nm at wavelengths below 1100 and 2 nm, above. As an example Fig. 1 shows the spectrum for glass *C* in the 300–900 nm range. The line strength of electric-dipole transitions between *J* initial $|(S,L)J\rangle$ and terminal $|(S',L')J'\rangle$ manifolds in the Judd-Ofelt treatment[7,8] may be written in the form[9]

$$S=\sum_{t=2,4,6}\Omega_t|\langle(S',L')J'\|U^{(t)}\|(S,L)J\rangle|^2, \qquad (1)$$

where Ω_t are the Judd-Ofelt intensity parameters (JO) and the $\langle\|U^t\|\rangle$ are the doubly reduced unit tensor operators calculated in the intermediate-coupling approximation.[7] Nine absorption bands lying between 350 and 900 nm and originating from the $^4I_{9/2}$ ground state were integrated, and these data together with the value for the Nd^{3+} concentration and the refractive index were fitted by a computerized least-squares program to yield the best-fit values for the Judd-Ofelt parameters Ω_2, Ω_4, and Ω_6.[7,8] It is known that the reduced matrix elements $\|U^t\|^2$ are almost independent of the ion environment. To estimate the Ω_t parameters we have utilized the values reported by Carnall, Crosswhite, and Crosswhite[10] for Nd^{3+} ions in LaF_3. The JO parameters obtained for the five samples are displayed in Table I. These values are in good agreement with those previously reported for the Nd^{3+} ion in different glass materials.[11–15] Ω_2 is the most sensitive to local structure and host composition, and its value is indicative of the amount of covalent bonding.[16] As can be seen in Table I the Ω_2 value is higher for the sample with the higher amount of phosphates which have a more covalent bonding character. Since the Ω_2 parameter reflects the asymmetry of the local environment at the Nd^{3+} site, a smaller value for the sample with the highest F/O ratio suggests a more centrosymmetric coordination environment.

TABLE I. Judd-Ofelt parameters (10^{-20} cm^2) calculated from the absorption spectra for Nd^{3+} (1 wt %).

Glass	Ω_2	Ω_4	Ω_6
A	2.33	2.78	4.43
B	2.19	2.80	4.38
C	2.12	2.79	4.46
D	1.83	2.84	4.33
E	1.84	2.84	4.32

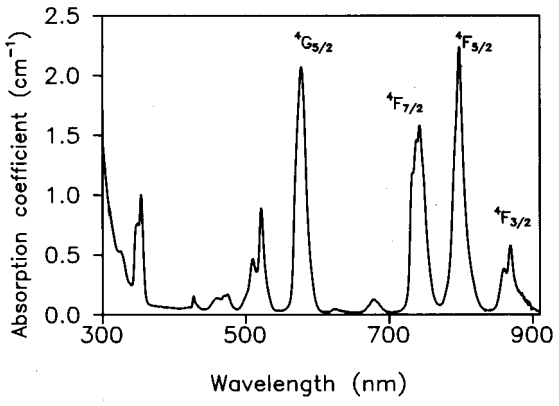

FIG. 1. Room-temperature absorption spectrum of Nd^{3+} ions in glass *C* doped with 1 wt % of Nd_2O_3.

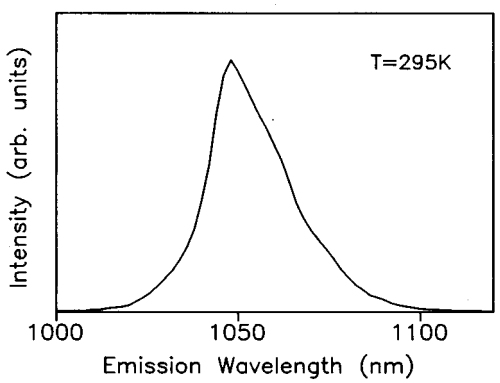

FIG. 2. Room-temperature fluorescence spectrum of the $^4F_{3/2} \rightarrow {}^4I_{11/2}$ transition Nd^{3+} (1 wt %) in glass *C* obtained under excitation with an argon laser.

B. Emission properties

The $^4F_{3/2} \rightarrow {}^4I_{11/2}$ steady-state fluorescence spectra at room temperature were measured for the five samples by exciting the samples with an argon laser. Figure 2 shows this emission spectrum for glass *C*. For all samples studied the emission bands are inhomogeneously broadened due to site-to-site variation in the local ligand field, and the wavelength of the fluorescence peak only shows a small variation ranging from 1048 to 1050 nm. Since the emission band is slightly asymmetric, an effective linewidth was determined by integrating the fluorescence line shape and dividing by the intensity at the peak fluorescence emission wavelength.[11]

The stimulated emission cross section can be determined from spectral parameters using[11]

$$\sigma_p(\lambda_p) = \frac{\lambda_p^4}{8\pi\ \mathrm{cn}^2 \Delta\lambda_{\mathrm{eff}}} A[(^4F_{3/2});(^4I_{11/2})], \tag{2}$$

where λ_p is the peak fluorescence wavelength, n is the refractive index, $\Delta\lambda_{\mathrm{eff}}$ is the effective linewidth of the transition and $A[(^4F_{3/2});(^4I_{11/2})]$ is the radiative transition probability for this transition.

The radiative transition probability from initial J' manifold $|(S',L')J'\rangle$ to terminal manifold $|(S,L)J\rangle$ is given by[9]

$$A[(S',L')J';(S,L)J] = \frac{64\pi^4 e^2}{3h(2J'+1)\lambda^3} n\left[\frac{(n^2+2)^2}{9}\right] \sum_{t=2,4,6} \Omega_t |\langle (S',L')J' \| U^{(t)} \| (S,L)J \rangle|^2, \tag{3}$$

where $n(n^2+2)^2/9$ is the local field correction for the Nd^{3+} ion in the initial J' manifold, n is the refractive index, λ is the wavelength of the transition, and J is the terminal manifold.

The radiative lifetime is related to the radiative transition probabilities by[9]

$$\tau_R = \left\{ \sum_{S,L,J} A[(S',L')J';(S,L)J] \right\}^{-1}. \tag{4}$$

The branching ratios can be obtained from the transition probabilities by using[9]

$$\beta[(S',L')J';(S,L)J] = \frac{A[(S',L')J';(S,L)J]}{\sum_{S,L,J} A[(S',L')J';(S,L)J]}. \tag{5}$$

The radiative transition probabilities and branching ratios for the fluorescence from the $^4F_{3/2}$ to the ^4I_J states were calculated by using the Judd-Ofelt parameters and Eqs. (3) and (5). These values are listed in Table II, together with the total spontaneous emission probability (W_R).

The resulting radiative lifetime τ_R and stimulated emission cross section for the $^4F_{3/2} \rightarrow {}^4I_{11/2}$ transition are presented in Table III together with the effective fluorescence linewidth. It is known that the effective linewidth is narrowed by using monovalent halide rather than divalent oxide anions. As can be seen in Table III, the narrowest effective linewidth corresponds to the sample with the highest content of fluoride ions. The stimulated emission cross section is determined by Ω_4, Ω_6, and the effective fluorescence linewidth. Because of the small variations of these quantities with the F/O ratio, the stimulated emission cross section is similar for the five samples. The radiative lifetime of the $^4F_{3/2}$ state only depends on the Ω_4 and Ω_6 parameters, which as shown in Table I, do not vary much with fluorine to oxygen ratio. However the correction for the local field at the Nd^{3+} site, introduces a dependence on the refractive index. Since the refractive index is smaller for the higher F/O ratio these samples show the longest lifetimes.

TABLE II. Branching ratios and spontaneous emission probability (W_R) for the $^4F_{3/2} \rightarrow {}^4I_J$ (J=9/2, 11/2, 13/2, 15/2) transitions of Nd^{3+} (1 wt %) in the five studied samples.

$^4F_{3/2} \rightarrow$	$^4I_{9/2}$	$^4I_{11/2}$	$^4I_{13/2}$	$^4I_{15/2}$	W_R (s^{-1})
Glass *A*	0.366	0.521	0.106	0.0056	1835
Glass *B*	0.369	0.519	0.106	0.0055	1808
Glass *C*	0.366	0.521	0.107	0.0056	1802
Glass *D*	0.372	0.517	0.105	0.0055	1767
Glass *E*	0.373	0.516	0.105	0.0055	1748

C. Lifetime results

The decays of the $^4F_{3/2} \rightarrow {}^4I_{11/2}$ transition were performed with a narrow band (0.08 cm^{-1} linewidth) tunable dye laser of 9 ns pulse width, exciting the sample at the $^4I_{9/2} \rightarrow {}^4G_{5/2}$ absorption band (575 nm). The measured fluorescence lifetime at room temperature of the five samples doped with 1 wt % of Nd_2O_3 are displayed in Fig. 3. As can be observed the lifetimes linearly increase when the fluorine to oxygen ratio increases.

The concentration dependence of the decays of the $^4F_{3/2}$ state between 0.5 and 5 wt % of Nd_2O_3 were obtained in the 4.2–300 K temperature range for glass *C*. The decays were found to be single exponentials at all temperatures and concentrations. This behavior may be due to the use of narrow-

TABLE III. Room-temperature emission properties of Nd^{3+} (1 wt %) in the five studied samples.

Glass	Refractive index	$\Delta\lambda_{\mathrm{eff}}$ (nm)	σ_p (10^{-20} cm^2)	τ_R (μs)	τ_{exp} (μs)
A	1.4589	28.50	2.56	545	472
B	1.4528	27.94	2.57	553	476
C	1.4477	27.84	2.60	555	482
D	1.4438	27.73	2.52	566	489
E	1.4396	27.70	2.53	572	494

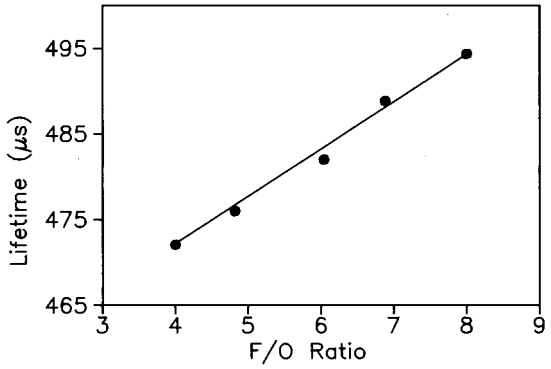

FIG. 3. Lifetimes of the $^4F_{3/2}$ state as a function of fluorine to oxygen ratio for the five glasses studied doped with 1 wt % of Nd_2O_3. Lifetimes were obtained by exciting at 575 nm and collecting the fluorescence at the emission peak of the $^4F_{3/2}\rightarrow{}^4I_{11/2}$ transition. Symbols stand for the experimental values, and solid line is the linear fit. Data correspond to room temperature.

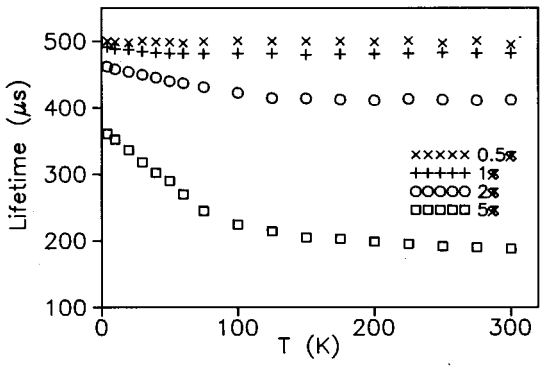

FIG. 5. Temperature dependence of the $^4F_{3/2}$ state lifetime of Nd^{3+} ions in glass *C*. (×) 0.5 wt %, (+) 1 wt %, (○) 2 wt %, and (□) 5 wt %. Lifetimes were obtained by exciting at 575 nm and collecting the fluorescence at the emission peak of the $^4F_{3/2}\rightarrow{}^4I_{11/2}$ transition.

band laser excitation. As an example Fig. 4 shows the room-temperature logarithmic plot of the experimental decays for glass *C* doped with 1, 2, and 5 wt % of Nd_2O_3. The lifetime values as a function of temperature are displayed in Fig. 5.

The fluorescence decays for the $^4F_{3/2}\rightarrow{}^4I_{11/2}$ emission were also measured as a function of the excitation wavelength along the $^4I_{9/2}\rightarrow{}^4G_{5/2}$ absorption band at 4.2 K. Figure 6 shows that the lifetime (which remains single exponential) does not exhibit a monotonic variation with wavelength as should correspond to the case of only one kind of statistical site distribution for Nd^{3+} ions.

IV. DISCUSSION

A. Absorption and equilibrium luminescence spectra

As can be seen in Fig. 5, at low temperatures and concentrations the lifetime nearly approaches the radiative lifetime, hence the rate of nonradiative decay by multiphonon emission must be small. As concentration rises the decays remain single exponential but a decrease in the experimental lifetimes is observed even at helium temperature. This behavior could be associated with a rapid energy diffusion between Nd^{3+} ions that can lead to a spatial equilibrium within the Nd^{3+} system. In the transfer rapid limit the donor transfer takes place so quickly that transfer times for different donor-acceptor pairs are averaged out and the whole system exhibits a simple exponential decay as is experimentally observed.[17,18] In order to investigate the energy migration process we have analyzed the relation between the absorption and equilibrium luminescence spectra. If the diffusion rate exceeds by far the excited-state decay rate, then, during a time equal to the lifetime of ions in the metastable level, thermodynamical equilibrium of the energy distribution of the excitations of the inhomogeneous ensemble of centers will be reached. The actual pattern of this distribution, $\rho(E,T,Z)$, and of the corresponding luminescence spectra depends neither on the excitation method nor on the migration parameters. It is only governed by the density of states $g(E)$, the temperature, and the fraction of excited centers Z.[19] In the limit of high temperature or low density, where the number of available quantum states is much greater than

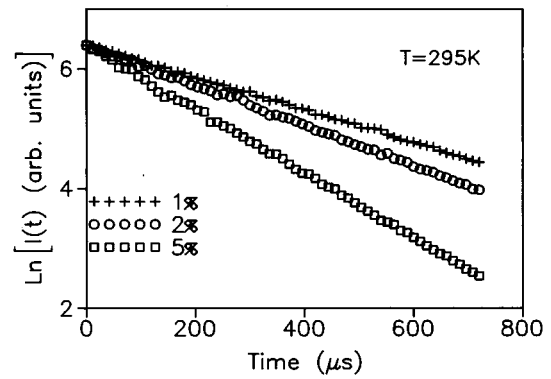

FIG. 4. Logarithmic plot of the fluorescence decays of the $^4F_{3/2}$ state for glass *C* doped with (+) 1, (○) 2, and (□) 5 wt % of Nd_2O_3. The decays were obtained by exciting at the $^4I_{9/2}\rightarrow{}^4G_{5/2}$ absorption band and monitored at the emission peak of the $^4F_{3/2}\rightarrow{}^4I_{11/2}$ transition. Data correspond to 295 K.

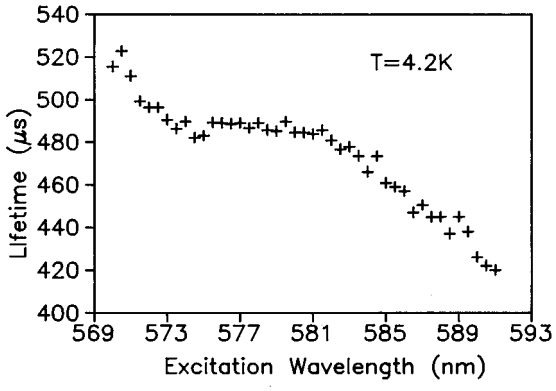

FIG. 6. Lifetimes of the $^4F_{3/2}$ state as a function of excitation wavelength along the $^4I_{9/2}\rightarrow{}^4G_{5/2}$ absorption band for glass *C* doped with 1 wt % of Nd_2O_3. Lifetimes were obtained at 4.2 K and collecting the fluorescence at the emission peak of the $^4F_{3/2}\rightarrow{}^4I_{11/2}$ transition.

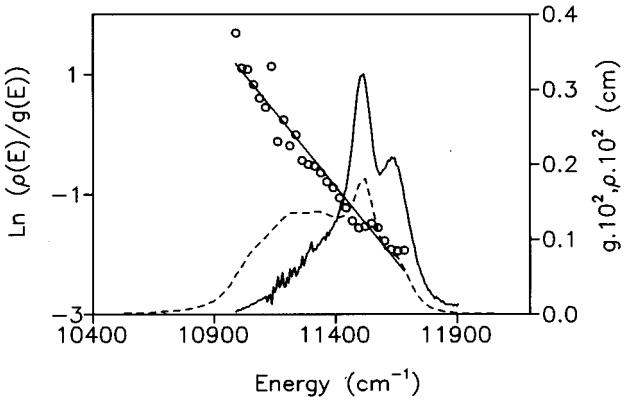

FIG. 7. Relation between the Nd^{3+} (1 wt %) absorption and luminescence spectra in glass *C*. (Solid line) $^4I_{9/2}\rightarrow{}^4F_{3/2}$ absorption band profile. (Dashed line) $^4F_{3/2}\rightarrow{}^4I_{9/2}$ luminescence band profile. (○), $\ln[\rho(E)/g(E)]$. $T=300$ K.

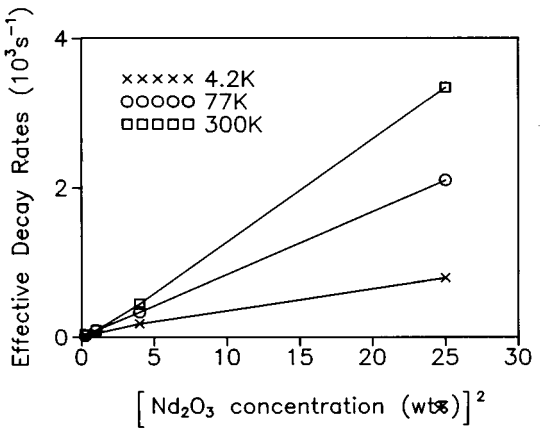

FIG. 8. Effective decay rates as a function of concentration at three different temperatures for glass *C*. (×) 4.2 K, (○) 77 K, and (□) 300 K. Solids lines are the fit to a linear dependence on the square of the Nd_2O_3 concentration.

the number of centers, the distribution becomes a Boltzman distribution and the equilibrium temperature can be obtained from the slope $\ln[\rho(E)/g(E)]$. Figure 7 shows the relation between the Nd^{3+} absorption and luminescence spectra for the $^4I_{9/2}\leftrightarrow{}^4F_{3/2}$ transition in glass *C* doped with 1 wt % of Nd_2O_3. The absorption cross section was taken proportional to $g(E)$ and the luminescence band profile proportional to $\rho(E)$; (profiles areas being normalized). The temperature derived from the slope calculation, account taken of the branching ratio for the $^4F_{3/2}\rightarrow{}^4I_{9/2}$ transition, was 300 K which agrees with the experimental temperature and demonstrates that the energy migration process drives the system of excited centers to thermal equilibrium.

B. Temperature-dependent concentration quenching of Nd^{3+} fluorescence

The lifetime of the $^4F_{3/2}$ state of Nd^{3+} ion in the doped glasses should be governed by the sum of probabilities for several competing processes such as radiative decay, nonradiative decay by multiphonon emission, and energy transfer to other Nd^{3+} ions. If one assumes that the purely radiative lifetimes τ_R of $^4F_{3/2}$ levels are independent of Nd^{3+} concentration and temperature, and disregarding multiphonon relaxation processes, the variations of the experimental lifetimes can be related with the nonradiative Nd-Nd relaxation processes by the simple relation:

$$\tau_{\text{exp}}^{-1}=\tau_R^{-1}+W_{\text{Nd-Nd}}(T). \tag{6}$$

Figure 8 shows the effective decay rates for glass *C* doped with 0.5, 1, 2, and 5 wt % of Nd_2O_3 at room, liquid-nitrogen, and liquid-helium temperatures. In this concentration range the effective decay rates show a linear dependence on the square of Nd_2O_3 concentration, indicating that Nd-Nd energy transfer probably occurs in the framework of a limited-diffusion regime. The diffusion is, however, fast enough to give exponential fluorescence decays.

A detailed study of the thermal dependence of lifetimes was presented in Fig. 5. These results suggest the presence of a quite strong thermal quenching mechanism between 4.2 and 100 K. If we disregard the multiphonon relaxation processes, relaxation via fast Nd-Nd difussion processes and subsequent deexcitation via energy sinks should be taken into account, as they occur even at low temperatures. Figure 9 shows the plot of $W_{\text{Nd-Nd}}(T)$ in the 4.2–100 K range for glass *C* doped with 2 and 5 wt % of Nd_2O_3. As can be observed the nonradiative rate has a nearly linear dependence with temperature.

It is well known that the Nd^{3+} fluorescence quenching depends on glass composition.[3] For this mixed fluorophosphate glass we could expect an intermediate behavior between a pure fluoride and a pure phosphate. In a previous work[6] some of the authors have investigated the temperature-dependent concentration quenching of Nd^{3+} fluorescence in three pure fluoride glasses. These fluoride glasses show a strong thermal quenching between 15 and 100 K where the nonradiative rates were found to increase with temperature as T^3, which is in agreement with a two-site nonresonant process in the short-wavelength regime as has been shown by Holstein, Lyo, and Orbach.[20] For comparison, Fig. 10 shows the thermal quenching of Nd^{3+} fluorescence in a pure fluoride glass and in the investigated fluorophosphate glass for

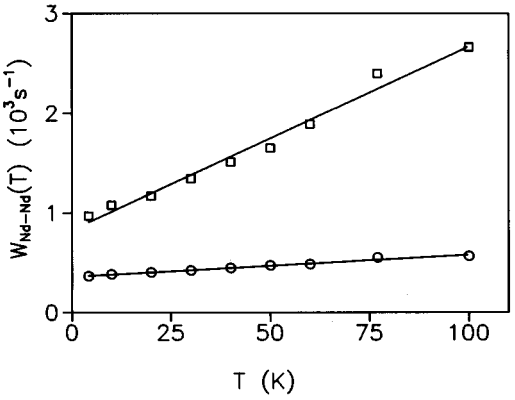

FIG. 9. Plot of the nonradiative Nd-Nd relaxation rate in the 4.2–100 K temperature range for glass *C* doped with a (○) 2, and (□) 5 wt % of Nd_2O_3. Symbols stand for the experimental values, and solid lines are the fit to a linear dependence on temperature.

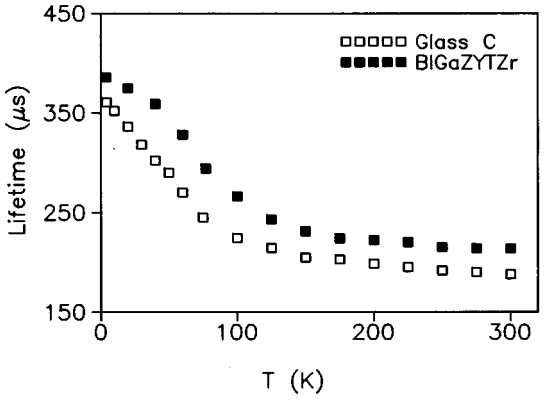

FIG. 10. Lifetimes as a function of temperature for Nd^{3+} ions (6.4×10^{20} cm^{-3}) in (■) a pure fluoride glass (BIGaZYTZr) and (□) in glass *C*. Lifetimes were obtained by exciting at 575 nm and collecting the luminescence at the emission peak of the $^4F_{3/2}\rightarrow{}^4I_{11/2}$ transition. Data for the fluoride glass correspond to Ref. 6.

the same concentration ($\approx6.4\times10^{20}$ ions/cm^3). As can be seen the fluorophosphate glass fails to show the temperature dependence of fluoride glasses in spite of its high fluorine content. The observed linear behavior of $W_{\text{Nd-Nd}}(T)$ with temperature can be related with the mixed nature of the fluorophosphate glass which seems to enhance the site-dependent effects. It is well known[20] that if the energy mismatch, ΔE, between nearby sites is large enough, one-phonon-assisted transfer is independent of ΔE and a linear dependence with temperature occurs. In order to investigate this hypothesis, we have performed fluorescence line narrowing experiments with Eu^{3+} in the same glass matrix. Although the local environment of Eu^{3+} may be altered from that of the Nd^{3+}-doped glass and therefore its value as a probe of intrinsic glass structure may be compromised, it is the variation of local environment from site to site which influences the energy-level positions and therefore the possibility of finding resonant or phonon-assisted energy transfer. Figure 11 shows the time evolution of the time-resolved resonant line-narrowed $^5D_0\rightarrow{}^7F_0$ emission band of Eu^{3+} in

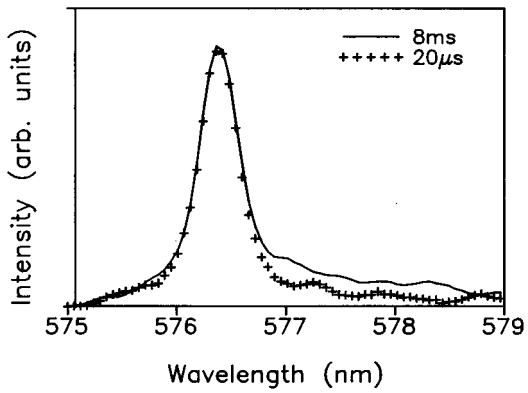

FIG. 11. Room-temperature fluorescence spectra of the $^5D_0\rightarrow{}^7F_0$ transition in glass *C* doped with 2 wt % of Eu_2O_3 obtained under excitation at 576.3 nm at two time delays after the laser pulse (+) 20 μs and (solid line) 8 ms.

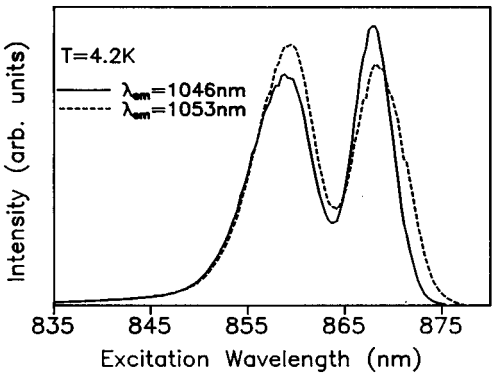

FIG. 12. Steady-state excitation spectra of $^4I_{9/2}\rightarrow{}^4F_{3/2}$ transition in glass *C* doped with 1 wt % of Nd_2O_3 for luminescence monitored at two different wavelengths within the $^4F_{3/2}\rightarrow{}^4I_{11/2}$ emission band. Measurements were performed at 4.2 K.

sample *C* doped with 2 wt % of Eu_2O_3. These spectra were obtained at room temperature and at two different time delays of 20 μs and 8 ms after the laser pulse, by exciting at the high energy side of the inhomogeneous absorption band. As can be observed, for the spectrum at 8 ms subsequent fluorescence from the acceptors ions tends to replicate the inhomogeneously broadened equilibrium emission profile, showing that transfer is not only to resonant sites but to the full range of sites within the inhomogeneous profile. This effect was found to be independent of the energy mismatch between the narrow peak and the barycenter of the equilibrium emission line showing that energy transfer is in this case a one-phonon-assisted process.

In the next section we shall see how lifetimes and homogeneous linewidths significantly depend on excitation wavelength showing the existence of a great variety of local fields environments at the activator ion in this mixed anion fluorophosphate glass matrix.

C. Site-dependent effects

Taking advantage of the tunability and narrow bandwidth of the Ti-sapphire ring laser as an excitation source for the $^4I_{9/2}\rightarrow{}^4F_{3/2}$, we have performed the excitation spectra of this transition collecting the luminescence at different wavelengths along the $^4F_{3/2}\rightarrow{}^4I_{11/2}$ transition. Figure 12 shows the steady-state excitation spectra obtained at two different emission wavelengths. As can be observed the spectrum slightly narrows and blueshifts for emission at the high-energy wing of the $^4F_{3/2}\rightarrow{}^4I_{11/2}$ emission.

The steady-state emission measurements were obtained for excitation into the $^4I_{9/2}\rightarrow{}^4F_{3/2}$ transition. Figure 13 shows the steady-state emission spectra obtained at different excitation wavelengths measured at 4.2 K. As can be observed the shape of the emission band changes as excitation goes to low energies through the low-energy Stark component of the $^4F_{3/2}$ doublet. Also as excitation wavelength increases, a strong narrowing and redshift of the emission spectra occur.

These results suggest that the fluorophosphate, which has a mixed nearest-neighbor coordination, contains (disregarding the geometry of the first coordination shell) a range of sites produced by the statistical effect of replacing a specified

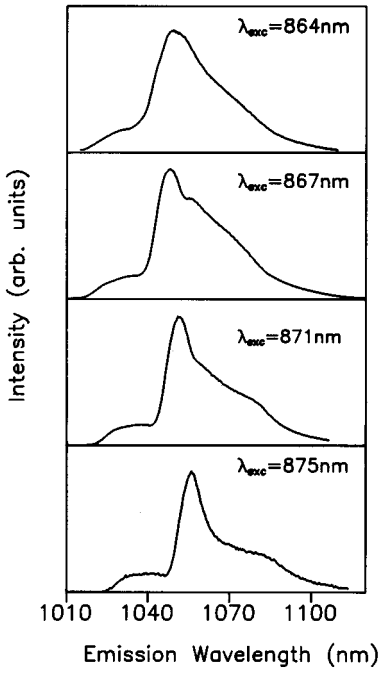

FIG. 13. Steady-state emission spectra of $^4F_{3/2}\rightarrow{}^4I_{11/2}$ transition in glass *C* doped with 1 wt % of Nd_2O_3 for different excitation wavelengths along the low-energy Stark component of the $^4F_{3/2}$ level. Measurements were performed at 4.2 K.

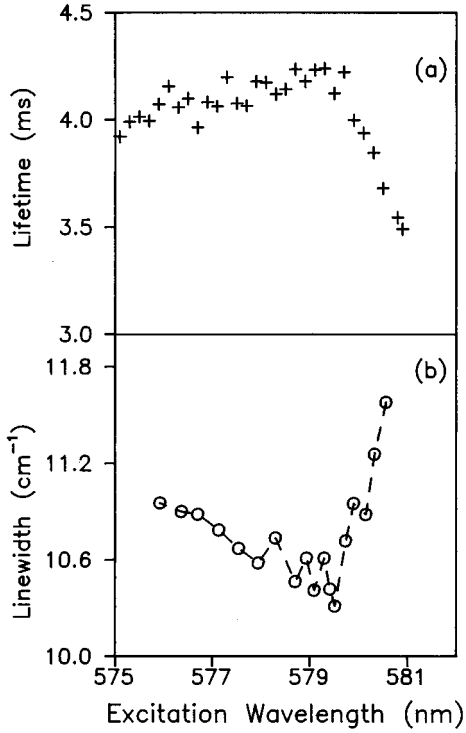

FIG. 14. (a) Lifetime of the line-narrowed fluorescence of the $^5D_0\rightarrow{}^7F_2$ hypersensitive transition of Eu^{3+} in glass *C* doped with 2 wt % of Eu_2O_3 obtained by exciting along the $^7F_0\rightarrow{}^5D_0$ absorption band. (b) Linewidth of the time-resolved resonant line-narrowed $^5D_0\rightarrow{}^7F_0$ emission band of Eu^{3+} as a function of excitation wavelength along the $^7F_0\rightarrow{}^5D_0$ absorption band in glass *C* doped with 2 wt % of Eu_2O_3. Measurements were performed at 1 ms after the laser pulse. Dashed line is only a guide for the eyes. Data correspond to 4.2 K.

number of one type of anion by another. This effect is felt through the different electronegativities of the anions and the strengths of their respective bonds with the Nd^{3+}.[21] Therefore at the shorter-wavelength excitations we should observe emissions from Nd^{3+} ions largely coordinated with fluorides whereas at the longer-wavelength excitations, emission from mainly oxide-coordinated Nd^{3+} ions should be dominant.[13] As Fig. 13 shows we failed to observe the narrowing effect by exciting at the high-energy side of the low-energy Stark component of the $^4F_{3/2}$ doublet. This is probably due to the presence of the aforementioned energy transfer between high- and low-energy Nd^{3+} sites and/or to some mixing with the emission produced by accidentally exciting low-field sites at the high-energy Stark component of the $^4F_{3/2}$ doublet.

As mentioned above, the site-dependent decay times for the $^4F_{3/2}\rightarrow{}^4I_{11/2}$ Nd^{3+} emission measured at 4.2 K (see Fig. 6) show that the lifetime, which displays a variation of about 100 μs, does not exhibit a monotonic change with wavelength. Moreover, longer decay times occur at shorter excitation wavelengths, and vice versa. These results point out to the existence of a strong site segregation for neodymium in these mixed fluorophosphate glasses, suggesting once more that those sites having predominantly fluoride coordination are excited at shorter wavelengths, whereas oxidiclike coordination sites are excited at longer ones.

In spite of the good resolution of our narrow bandwidth Ti-sapphire ring laser as an excitation source for the $^4I_{9/2}\rightarrow{}^4F_{3/2}$ transition, accidental coincidences of the Stark components belonging to different sites mainly containing fluoride or oxide coordinators, may limit the expected site-selection process in the emission spectra (Fig. 13), if compared with lifetimes. In order to overcome these difficulties and to address the influence of the local coordination ions on the optical properties of rare earths in these fluorophosphate glasses we have performed fluorescence line-narrowing spectroscopy on Eu^{3+}. It is well known[14,22,23] that the $^5D_0\leftrightarrow{}^7F_0$ transition of Eu^{3+} is ideally suited for a study of line broadening in glasses because a single transition between nondegenerate levels can be studied with no overlapping from neighboring crystal-field components. Moreover, the energy gap between $^5D_0$ state and the next lower $^7F_6$ state is about ten times the highest involved phonon energy. Therefore, the probability of nonradiative deexcitation of $^5D_0$ state by multiphonon processes is very small. At low dopant concentrations and temperatures, cross relaxation via ion-ion interaction can be disregarded and the measured lifetimes of the $^5D_0$ state can be considered mainly radiative. Thus their dependence with excitation wavelength should parallel the variations of the electric dipolar transition rates.[24] On the other hand, ions in different environments have different electron-phonon coupling strengths and therefore will have different homogeneous linewidths. Because homogeneous linewidth, $\Delta\nu$, and relaxation (or dephasing) time τ are related by the expression $\Delta\nu=(2\pi\tau)^{-1}$, we can obtain complementary information by working either in the frequency or the time domain.[25] Figure 14(a) shows the results obtained for the decay of the line-narrowed fluorescence of the $^5D_0\rightarrow{}^7F_2$ hypersensitive transition of Eu^{3+} which is very sensitive to small changes in the chemical surroundings of

the ion.[26] As can be observed, the dependence on excitation wavelength (by exciting along the $^7F_0 \rightarrow {}^5D_0$ absorption band) of the Eu^{3+} lifetime presents similar features (see Fig. 6) than the fluorescence decay for the $^4F_{3/2} \rightarrow {}^4I_{11/2}$ emission of Nd^{3+} as a function of the excitation wavelength along the hypersensitive $^4I_{9/2} \rightarrow {}^4G_{5/2}$ transition. As it is well known[12] a larger transition probability of this hypersensitive transition corresponds to an increase of covalent bonding, and because the field strength of the rare-earth ligand increases by divalent oxide anions rather than monovalent fluoride ions, the distribution of lifetimes as a function of excitation energy gives us a picture of the type of anion coordination around the rare earth. Therefore, at shorter wavelengths we have an enhanced probability of fluoride-coordinated rare-earth ions whereas at longer wavelengths oxide coordinated sites become dominant. This lifetime result is mirrored by the measured linewidth of the time-resolved resonant line-narrowed $^5D_0 \rightarrow {}^7F_0$ emission band of Eu^{3+} as a function of excitation wavelength along the $^7F_0 \rightarrow {}^5D_0$ absorption band. Figure 14(b) shows this wavelength dependence obtained at 4.2 K and 1 ms after the laser pulse in sample *C* doped with 2 wt % of Eu_2O_3. At this concentration and temperature, energy transfer between Eu^{3+} ions can be neglected. Although the spectral width of the laser pulse (0.08 cm^{-1}) could be much narrower than the expected homogeneous linewidth we were limited by the spectral resolution (3 cm^{-1}) of the optical multichannel analyzer. Nevertheless as the results are good enough in order to be compared with lifetimes we made no deconvolution in the resulting spectra. It is clear from this figure that homogeneous linewidths are dominated by lifetime broadening caused by rapid phonon relaxation processes and therefore also yield a very valuable information about the strength of ion-phonon coupling in this glass matrix, confirming once more that the less efficient and more distorted local environments correspond to the oxide-coordinated sites. Our results are somewhat different from those found in other fluorophosphate glasses.[13] In our system there is a clear crossover between the behavior of fluorinelike and oxygenlike coordination anions. This sharp segregation of sites with relatively large differences in electron-phonon couplings should also give a broad energy distribution for the energy levels of Nd^{3+}, thus reinforcing the hypothesis that energy transfer between Nd^{3+} ions takes place in these glasses mainly by a one-phonon process.

V. CONCLUSIONS

(i) From the steady-state optical-absorption measurements the Judd-Ofelt parameters were derived and used to calculate the $^4F_{3/2} \rightarrow {}^4I_{11/2}$ stimulated emission cross section and the $^4F_{3/2}$ radiative lifetime for Nd^{3+} in five samples with different fluorine to oxygen ratios. The Ω_2 parameter decreases as the fluorine to oxygen ratio increases, indicating a more covalent bonding in glasses with a lower F/O ratio. The effective linewidth of the $^4F_{3/2} \rightarrow {}^4I_{11/2}$ transition decreases when the fluorine to oxygen ratio increases.

(ii) The decays of the $^4F_{3/2}$ state were found to be single exponential for all temperatures and concentrations. For the samples doped with 1 wt % of Nd_2O_3 the lifetimes were found to be linear dependent on the F/O ratio.

(iii) Quenching of the Nd^{3+} fluorescence by Nd-Nd interactions is already present at concentrations higher than 1 wt %. As the concentration rises the decay remains single exponential but a decrease in the experimental lifetime is observed even at helium temperature, showing that relaxation via fast Nd-Nd diffusion processes occurs.

(iv) From the relation between the absorption and luminescence spectra, the thermodynamical equilibrium temperature of the energy distribution of the excitations has been estimated. The obtained result is in agreement with the experimental temperature demonstrating that the energy migration process drives the system of excited centers to thermal equilibrium.

(v) The observed linear behavior of $W_{\text{Nd-Nd}}(T)$ with temperature between 4.2 and 100 K can be related with the mixed nature of the fluorophosphate glass which enhances the site-dependent effects giving a broad energy distribution for the energy levels of Nd^{3+} and allowing for one-phonon-assisted ion-ion cross relaxation processes.

(vi) The influence of the local coordination ions on the optical properties of Eu^{3+} in these fluorophosphate glasses investigated by fluorescence line-narrowing spectroscopy shows the existence of a clear crossover between the behavior of fluorinelike and oxygenlike coordination anions. This sharp segregation of sites with relatively large differences in electron-phonon couplings should give a broad energy distribution of energy levels in the case of Nd^{3+} doped glass.

ACKNOWLEDGMENTS

The authors wish to thank Dr. Marvin J. Weber for helpful comments and appreciate his critical reading of the manuscript. This work was supported by the Comisión Interministerial de Ciencia y Tecnología (CICYT) of the Spanish Government (Ref. MAT93-0434), and Basque Country University (Ref. EB148/93).

[1] D. Ehrt and W. Seeber, J. Non-Cryst. Solids **129**, 19 (1991).
[2] M. J. Weber, C. Layne, R. Saroyan, and D. Milam, Opt. Commun. **18**, 171 (1976).
[3] S. E. Stokowski, in *Laser, Spectroscopy and New Ideas*, edited by W. M. Yen and M. D. Levensen (Springer-Verlag, Berlin, 1987).
[4] M. J. Weber, J. Non-Cryst. Solids **47**, 117 (1982).
[5] M. J. Weber, J. Non-Cryst. Solids **123**, 208 (1990).
[6] R. Balda, J. Fernández, A. Mendioroz, J. L. Adam, and B. Boulard, J. Phys. Condens. Matter **6**, 913 (1994).
[7] B. R. Judd, Phys. Rev. **127**, 750 (1962).
[8] G. S. Ofelt, J. Chem. Phys. **377**, 511 (1962).
[9] W. F. Krupke, IEEE J. Quantum Electron. **QE-10**, 450 (1974).
[10] W. T. Carnall, H. Crosswhite, and H. M. Crosswhite (unpublished).
[11] R. R. Jacobs and M. J. Weber, IEEE J. Quantum Electron. **QE-12**, 102 (1976).

[12] R. Reisfeld and C. K. Jorgensen, *Lasers and Excited States of Rare Earths* (Springer-Verlag, Berlin, 1977).
[13] C. Brecher, L. A. Riseberg, and M. J. Weber, Phys. Rev. B **18**, 5799 (1978).
[14] M. J. Weber, in *Laser Spectroscopy of Solids*, edited by W. M. Yen and P. M. Selzer (Springer-Verlag, Berlin, 1981), pp. 189–239.
[15] A. Tesar *et al.*, Opt. Mater. **1**, 217 (1992).
[16] C. K. Jørgensen and R. Reisfeld, J. Less-Common Met. **93**, 107 (1983).
[17] D. L. Huber, in *Laser Spectroscopy of Solids* (Ref. 14), p. 83.
[18] M. J. Weber, Phys. Rev. **4**, 2932 (1971).
[19] T. T. Basiev, V. A. Malyshev, and A. K. Przhevuskii, in *Spectroscopy of Solids Containing Rare-Earth Ions*, edited by A. A. Kapliansky and R. M. Macfarlane (North-Holland, Amsterdam, 1987), p. 275.
[20] T. Holstein, S. K. Lyo, and R. Orbach, in *Laser Spectroscopy of Solids* (Ref. 14), p. 40.
[21] C. Brecher, L. A. Riseberg, and M. J. Weber, J. Lumin. **18/19**, 651 (1979).
[22] R. M. Macfarlane and R. M. Shelby, J. Lumin. **36**, 179 (1987).
[23] R. Balda, J. Fernández, H. Eliers, and W. M. Yen, J. Lumin. **59**, 81 (1993), and references therein.
[24] C. Brecher and L. A. Riseberg, Phys Rev. B **21**, 2607 (1980).
[25] P. M. Selzer, in *Laser Spectroscopy of Solids* (Ref. 14), p. 113.
[26] C. K. Jørgensen and B. R. Judd, Mol. Phys. **8**, 291 (1964).